nature communications

Article

https://doi.org/10.1038/s41467-025-64160-0

LAT1-NRF2 axis controls sFlt-1/PlGF imbalance and oxidative stress in preeclampsia

Received: 21 March 2024

Accepted: 9 September 2025

Published online: 14 October 2025

Check for updates

Sebastian Granitzer[1,2,11], Raimund Widhalm[1,2,11], Isabella Ellinger[3], Harald Zeisler[4], Martin Forsthuber[2], Philipp Foessleitner[4,5], Elisabeth Geschrey[5], Leila Saleh[4], Martin Knöfler[4], Gernot Desoye[6], Paul Ettel[2], Thomas Weichhart[2], Laszlo Musiejovsky[7,8], Gernot Schabbauer[7,8], Hans Salzer[9], Margit Rosner[2], Markus Hengstschläger[2] & Claudia Gundacker[2,10]

Preeclampsia (PE) is a complex disease with unclear etiology. It is the most dangerous human pregnancy disease, causing morbidity and mortality in thousands of women and newborns worldwide. The soluble fms-like tyrosine kinase-1 (sFlt-1) to placental growth factor (PlGF) ratio is currently the best and only predictive biomarker. The higher the ratio, the more likely the pregnant women will develop PE. The molecular mechanism underlying the increased sFlt-1/PlGF ratio is not known. Here, we show that amino acid transporter LAT1 (*SLC7A5*) and transcription factor NRF2 regulate this ratio via a previously unknown mechanism to produce sFlt-1 and PlGF in an anti-angiogenic ratio as observed in PE. In addition, we show that PE-associated oxidative stress, whose origin was unknown, is a secondary phenomenon caused by reduced NRF2 and LAT1 activity. The interdependence of the involved proteins, including also ATF4, Flt-1 and Akt, indicates that any disruption of the interaction would ultimately lead to a PE-like phenotype.

Preeclampsia (PE), a complex disease of human pregnancy, is a leading cause of maternal and neonatal morbidity and mortality[1,2]. The treatment options are limited, and in many cases the only way to save the lives of women and fetuses is – often premature – delivery. The long-term health effects include cardiovascular and metabolic diseases in later life of both women and infants, and neurodevelopmental disorders of infants[3,4].

PE is diagnosed by (sudden) onset of maternal hypertension combined with at least one other complication, e.g., maternal organ dysfunction, and proteinuria[4]. There are striking differences in the severity and progression of the disease[1]. The currently best predictive biomarker is the increased soluble fms-like tyrosine kinase-1 (sFlt-1) to placental growth factor (PlGF)[5] ratio (Supplementary Fig. 1A). PlGF is a member of the vascular endothelial growth factor (VEGF) family and predominantly expressed in the placenta[6]. Flt-1, also known as VEGF receptor (VEGFR)1, is able to antagonise pro-angiogenic PlGF or VEGF-A in its soluble form sFlt-1, resulting in less Flt-1 autophosphorylation and impaired downstream signalling (e.g., PIK3/Akt)[7,8].

[1]Karl-Landsteiner Private University for Health Sciences, Krems, Austria. [2]Institute of Medical Genetics, Medical University of Vienna, Vienna, Austria. [3]Institute for Pathophysiology and Allergy Research, Medical University of Vienna, Vienna, Austria. [4]Department of Obstetrics and Gynecology, Reproductive Biology Unit, Placental Development Group, Medical University of Vienna, Vienna, Austria. [5]Department of Gynecology and Obstetrics, University Hospital St. Pölten, St. Pölten, Austria. [6]Department of Obstetrics and Gynecology, Medical University of Graz, Graz, Austria. [7]Institute for Vascular Biology, Medical University Vienna, Vienna, Austria. [8]Christian Doppler Laboratory Arginine Metabolism in Rheumatoid Arthritis and Multiple Sclerosis, Vienna, Austria. [9]Clinic for Pediatrics and Adolescent Medicine, University Clinic Tulln, Tulln, Austria. [10]Exposome Austria, Research Infrastructure and National EIRENE Hub, Vienna, Austria. [11]These authors contributed equally: Sebastian Granitzer, Raimund Widhalm. e-mail: claudia.gundacker@meduniwien.ac.at

The etiology of PE is unclear[1,2]. In preeclamptic placentas insufficient spiral artery remodelling occurs[9]. This leads to high blood pressure in the intervillous space (Supplementary Fig. 1B) and uteroplacental malperfusion. Both factors stress the syncytiotrophoblast (STB), the outer epithelial cell layer covering the placental villi that are in contact with maternal blood[1,2]. Oxidative stress is one of the hallmarks of the stressed STB[4]. It is unknown whether the PE-related oxidative stress of placental cells is a cause or a consequence of the disease[10].

Cellular oxidative stress is primarily controlled by the nuclear factor erythroid 2–related factor (NRF)2/Kelch-like ECH-associated protein (Keap)1 system. When cellular oxidative stress increases, cysteine residues on Keap1 are oxidised, which leads to the release of NRF2[11]. Unbound NRF2 becomes phosphorylated and migrates to the nucleus where it acts as a transcription factor for numerous genes (Supplementary Fig. 2), including ABC transporters (e.g., multidrug resistance-associated protein (MRP)1) and proteins essentially required in glutathione (GSH)-driven redox homeostasis[12]. Metabolism continuously generates reactive oxygen species (ROS). This requires a constant and rapid supply of GSH, the most abundant intracellular low molecular weight thiol compound that protects against oxidative damage[13,14] (Supplementary Fig. 2). The specific conditions under which NRF2 is involved in the pathogenesis of PE are unclear[3,15].

GSH synthesis depends on the availability of its precursor amino acids. The functionally relevant amino acid of the tripeptide GSH is cysteine, as its sulfhydryl group is involved in redox and conjugation reactions[16]. L-type amino acid transporter (LAT)1 (*SLC7A5*) is abundantly expressed at the apical side of the STB[17]. Along with leucine, LAT1 mainly imports methionine that serves via the S-adenosylmethionine (SAM) cycle as intracellular cysteine reservoir[18,19]. Under amino acid deprivation activating transcription factor (ATF)4 is upregulated to induce the transcription of antioxidant genes[20,21]. ATF4, mainly involved in mitigating ER stress and proper function of amino acid metabolism, has higher transcriptional activity in preeclamptic placentas, and downregulates PlGF expression[22].

Here, primary human trophoblast cells (hTCs) and HTR-8/SVneo cells, an immortalised first trimester trophoblast cell line[23], were used to investigate how LAT1 and the NRF2/Keap1 system interact and how this interaction affects the sFlt-1/PlGF ratio indicative of a PE-like phenotype. We show that LAT1 deficiency causes an ATF4-mediated upregulation of sFlt-1, and downregulation of PlGF, resulting in lower Flt-1 signalling. Lower Flt-1-related Akt activation reduces NRF2 activity, ultimately increasing cellular susceptibility for oxidative stress. The lack of LAT1 also leads to reduced import of methionine, an important source of cysteine, which is required for GSH synthesis. Key findings on this molecular mechanism were confirmed in a mouse model using a LAT1-specific inhibitor. We further show that the anti-angiogenic expression of sFlt-1 and PlGF by trophoblast cells makes primary placental endothelial cells (PLECs) more susceptible to oxidative stress via paracrine signalling. Taken together, this study reveals a so far unknown molecular mechanism that describes how PE-derived trophoblast cells are generating anti-angiogenic conditions.

Results

Functional characterisation of PE-derived trophoblasts

Similar to the increased sFlt-1/PlGF ratio observed in the serum of women affected by PE[5], primary human trophoblast cells (hTCs) isolated from PE placentas showed an increased sFlt-1/PlGF ratio (Fig. 1A) by the release of more sFlt-1 and less PlGF (Supplementary Fig. 3A); the corresponding mRNA levels matched well (Supplementary Fig. 3B).

The elevated sFlt-1/PlGF ratio led to reduced Flt-1 signalling demonstrated by less phosphorylated Flt-1 and consequently less phosphorylated Akt, a downstream target of Flt-1 (Fig. 1B). In accordance with lower *PGF* (PlGF) transcription, *ATF4* expression was upregulated in hTCs from PE placentas (Fig. 1C), likely because of impaired amino acid uptake (Fig. 1D). The diminished uptake of leucine and methionine in hTCs from PE placentas fitted well with the reduced expression of uptake transporter LAT1 on the protein (Fig. 1E) and mRNA (Fig. 1H) level.

Methylmercury (MeHg) bound to cysteine is another substrate of LAT1[24], as the compound structurally mimics methionine[25]. In accordance with reduced LAT1 function, PE-derived hTCs showed lower cellular Hg levels (Fig. 1F). Furthermore, MeHg is a well-known oxidative stressor, also of placental cells[26] and we observed increased sensitivity of PE-derived hTCs to the metal (Fig. 1G). This finding is supported by the lower levels of *NFE2L2* (encodes NRF2) (Fig. 1H), which is normally activated in response to oxidative stress. In line with lower NRF2, mRNA levels of its target *ABCC1* (encodes MRP1) were also reduced (Fig. 1H).

Importantly, all three genes (*SLC7A5, NFE2L2*, *ABCC1*) could be upregulated by MeHg in healthy but not in PE-derived hTCs (Fig. 1H) clearly indicating the higher vulnerability of PE-derived cells to oxidative stress. In addition, *SLC7A5* and *NFE2L2* in whole placental tissue are strongly correlated, regardless of whether PE is present or not (Fig. 1I), indicating a disease-independent relationship between LAT1 and NRF2.

LAT1 and NRF2 link oxidative stress and amino acid response

To determine whether the connected expression of LAT1 and NRF2, and the concomitantly reduced LAT1 and NRF2 expression in PE-derived trophoblasts are mechanistically connected, trophoblast cell line HTR-8/SVneo was used. We individually depleted *SLC7A5* and *NFE2L2* by siRNA-mediated gene silencing and analysed their mutual regulation.

Surprisingly, we found LAT1 and NRF2 to regulate each other. NRF2 deficiency strongly reduced promoter activity of MRP1 (this was expected) but also of *SLC7A5* (Fig. 2A). In return, LAT1 silencing decreased *NFE2L2* promoter activity, its gene expression, and nuclear NRF2 activity (Fig. 2B) suggesting LAT1 as a hitherto unknown regulator of NRF2. Accordingly, we saw no reciprocal regulation between MRP1 and NRF2 (Supplementary Fig. 4) or MRP1 and LAT1 (Supplementary Fig. 5A), but reduced expression of NRF2 target *ABCC1* (MRP1) during LAT1 deficiency (Supplementary Fig. 5A). Lower NRF2 function in LAT1 deficient cells was not mediated by enhanced levels of NRF2's negative regulator, Keap1 (Supplementary Fig. 5B). This Keap1 independent influence on NRF2 during LAT1 depletion was further demonstrated by concomitant silencing of Keap1 (NRF2 fully active). If Keap1 was depleted, the remaining NRF2 activity in LAT1 deficient cells was still able to transcriptionally activate MRP1 expression (Fig. 2C).

Depletion of LAT1 or NRF2 induced cellular oxidative stress as indicated by the lower ratio of GSH to glutathione disulphide (GSSG) (Fig. 2D). Treatment with GSH precursor cysteine (as N-acetyl cysteine (NAC), or methionine) reduced the oxidative stress. In LAT1 deficient cells only NAC treatment was able to restore the GSH/GSSG ratio to the levels of control cells. In case of NRF2 depletion, the GSH/GSSG ratio could not be increased by either compound. Furthermore, total intracellular GSH levels were reduced upon depletion of LAT1 and NRF2 (Fig. 2E). In agreement with this, we also found lower mRNA levels of the GSH synthesising protein Glutamate-cysteine ligase modifier subunit (GCLM) in LAT1 depleted cells (Fig. 2F). The lower total GSH levels in LAT1 deficient cells could also be due to a lower availability of amino acids. In fact, besides leucine, methionine levels were also reduced after LAT1 silencing (Fig. 2G).

Methionine starvation further induced *ATF4* expression (Fig. 2H), as did cysteine, arginine, and lysine starvation, but not leucine (Supplementary Fig. 6).

LAT1 and NRF2 regulate the sFlt-1/PlGF ratio via ATF4

In a next step, we identified ATF4 in the regulation of the angiogenesis modulating factors sFlt-1 and PlGF. ATF4 expression could be induced

https://doi.org/10.1038/s41467-025-64160-0

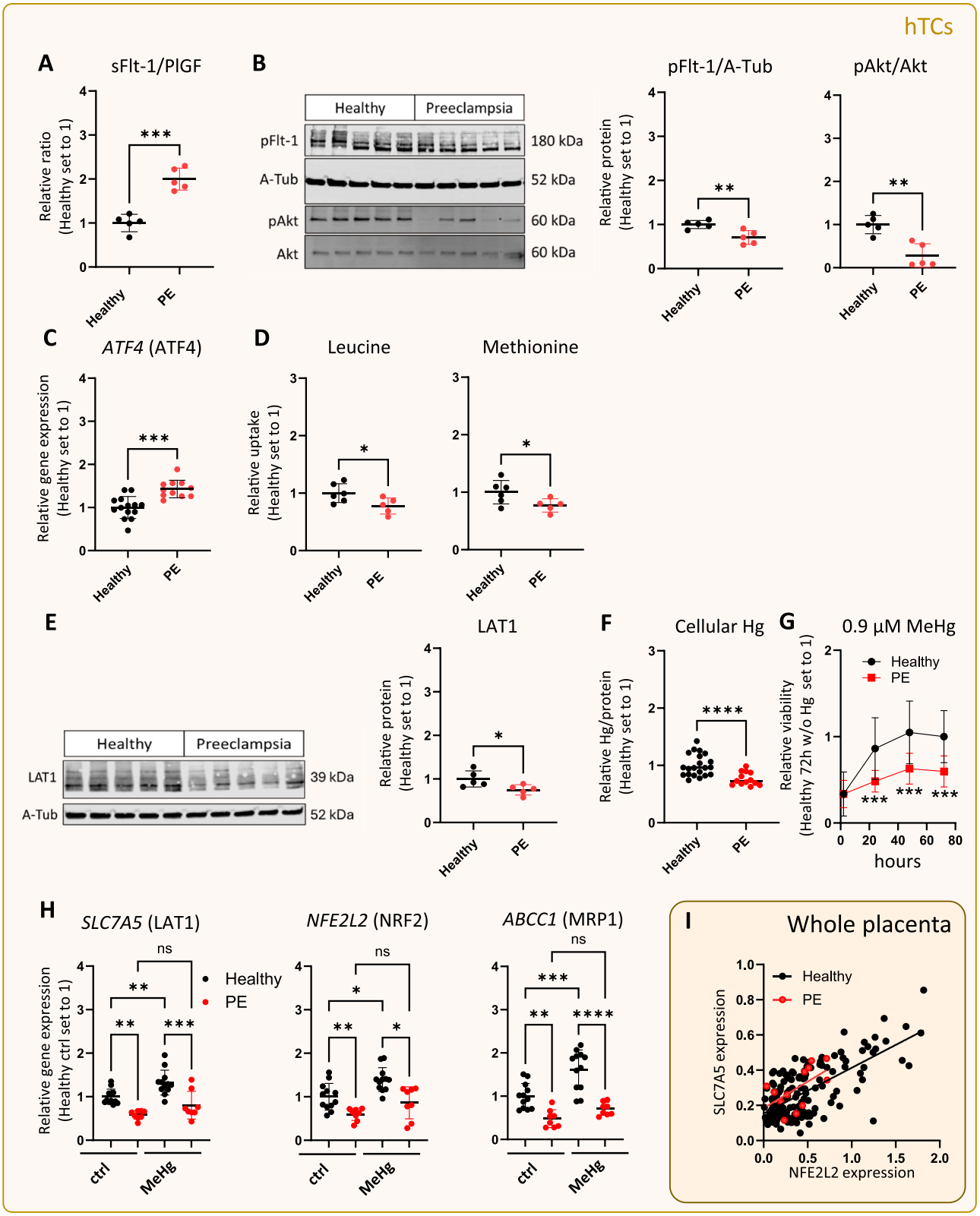

with Tunicamycin, which increased Flt-1 and decreased PlGF gene expression, causing an elevated *Flt1*/*PGF* mRNA ratio (Fig. 3A). Depletion of *ATF4* had the opposite effect (less Flt-1 and more PlGF gene expression), resulting in a lower *Flt1*/*PGF* mRNA ratio that was unaffected by Tunicamycin treatment (Fig. 3A). Like PE-derived hTCs, LAT1 and NRF2 deficient HTR-8/SVneo cells had higher *ATF4* mRNA levels than controls (Fig. 3B). In line with this, we observed on the mRNA level (Supplementary Fig. 7) and the protein level (Fig. 3C) that LAT1 and NRF2 depletion increased *Flt1* and decreased *PGF* gene expression, respectively. This resulted in an elevated sFlt-1/PlGF ratio, resembling the PE phenotype (Fig. 3C). Accordingly, depletion of ATF4 reduced the sFlt-1/PlGF ratio, even when LAT1 was concomitantly silenced (Fig. 3D). The increased PE-like sFlt-1/PlGF ratio induced by LAT1 and NRF2 deficiency could also be reduced by overexpression (OE)

Fig. 1 | Impaired oxidative stress response of primary human trophoblasts (hTCs) from preeclamptic (PE) placentas. A sFlt-1/PlGF ratio in cell culture medium from hTCs from healthy and PE placentas. **B** Protein levels of phosphorylated Flt-1, and phosphorylated and total Akt in hTCs derived from healthy or PE placentas. **C** *ATF4* (ATF4) mRNA levels in hTCs from healthy and PE placentas. **D** Leucine and methionine uptake in hTCs from healthy and PE placentas. **E** LAT1 protein levels in hTCs from healthy and PE placentas. **F** Cellular Hg levels in hTCs from healthy and PE placentas after 5 h treatment with 0.9 μM methyl mercury (MeHg). **G** Viability of hTCs isolated from healthy and PE placentas after treatment with 0.9 μM MeHg. **H** Gene expression of *SLC7A5, NFE2L2*, and *ABCC1* of hTCs from healthy and PE placentas after 5 h exposure to 0.9 μM MeHg. **I** Correlation of *SLC7A5* (LAT1) and *NFE2L2* (NRF2) gene expression in whole placenta lysates. Data represent mean value ± SD. **A**, **B** Healthy ($N = 5$), PE ($N = 5$); **C** Healthy ($N = 14$), PE= ($N = 11$); **D** Healthy ($N = 6$), PE ($N = 5$); **E** Healthy ($N = 5$), PE ($N = 5$); **F** Healthy ($N = 21$), PE ($N = 13$); **G** Healthy ($N = 20$), PE ($N = 13$), **H** (Healthy w/o MeHg ($N = 12$), Healthy with MeHg ($N = 8$), PE w/o MeHg ($N = 12$), PE with MeHg ($N = 8$), **I** $N = 178$. **I** Healthy $N = 166$, $R_s = 0.51$, $P \leq 0.0001$; PE $N = 12$, $R_s = 0.60$, $P = 0.0428$; overall $N = 178$, $R_s = 0.52$, $P \leq 0.001$; $^*P < 0.05$, $^{**}P < 0.01$, $^{***}P < 0.001$, $^{****}P < 0.0001$. Two-sided unpaired *t* test was used in (**A**–**F**). Two-sided unpaired *t* test was used in (**G**) for each time point. ANOVA followed by Tukey´s multiple comparisons test was used in (**H**). The Spearman correlation was used for the calculation in (**I**).

of NRF2, or LAT1, respectively (Fig. 3E). Confirmation of gene silencing and OE was done on mRNA and protein level (Supplementary Fig. 8).

Next, we determined whether the increased sFlt-1/PlGF ratio during LAT1 and NRF2 deficiency was a direct result of oxidative stress that occurred during these conditions. Therefore, we treated HTR-8/SVneo cells with various oxidative stressors (MeHg, Menadione, H_2O_2, and BSO). Although all these compounds were able to decrease the GSH/GSSG ratio, they did not increase the sFlt-1/PlGF ratio (Supplementary Fig. 9).

Afterwards, we treated cells during LAT1 deficiency with MeHg and NAC to determine whether oxidative stress in PE (indicated by the GSH/GSGG ratio) is a secondary effect of decreased LAT1 function or a primary etiological factor. The role of NRF2 was not investigated as NAC failed to reduce oxidative stress during NRF2 deficiency (Fig. 2D). We hereby show that independent of cellular oxidative stress, the sFlt-1/PlGF ratio was only increased in LAT1 deficiency (Fig. 3F).

To demonstrate the crucial role of impaired LAT1 function in PE in vivo, we used a mouse model, applying the LAT1-specific inhibitor JPH203. We injected the inhibitor into pregnant mice over a 72-hour period (from gestational day 14), which resulted in higher oxidative stress in the placenta (Fig. 3G), increased *ATF4* and decreased *NFE2L2* (NRF2) levels in the placenta (Fig. 3H), as well as a phenotype in pregnant mice similar to PE, namely maternal proteinuria (Fig. 3I) and an increased sFlt-1/PlGF-2 ratio in maternal blood (Fig. 3J). The increased sFlt-1/ PlGF-2 ratio further favoured conditions of impaired Flt-1 signalling resulting in decreased Akt phosphorylation in placentas from JPH203-treated pregnant mice (Supplementary Fig. 10). When we employed JPH203 (and BCH, another LAT1 inhibitor) in hTCs and HTR-8/SVneo cells, we saw a similar pattern as in PE-derived trophoblasts: Decreased amino acid (and MeHg) uptake, higher ATF4 and lower *NFE2L2* expression, an elevated sFlt-1/PlGF ratio, and decreased phosphorylation of Flt-1, and Akt (Supplementary Fig. 11, Supplementary Fig. 12).

Reduced Flt-1 signalling impairs NRF2 function

We wanted to determine how the increased sFlt-1/PlGF ratio during LAT1 deficiency affects Flt-1 and its downstream signalling. As expected, silencing of LAT1 resulted in less phosphorylated Flt-1 and decreased Akt phosphorylation (Fig. 4A). Treatment with the Akt activator SC79, ameliorated the decrease of Flt-1 and Akt phosphorylation during LAT1 depletion (Fig. 4A). If Akt was inhibited by Wortmannin, we observed a similar reduction in *NFE2L2* expression as during LAT1 deficiency that was accompanied by more oxidative stress, i.e., a lower GSH/GSSG ratio (Fig. 4B).

Independent of proper NRF2 activation via Akt, LAT1 deficiency led to more oxidative stress. While SC79 was able to elevate *NFE2L2* levels in control and LAT1 deficient cells, it could not rescue the decreased GSH/GSSG ratio during LAT1 silencing (Fig. 4C).

Next, we wanted to see if the downstream signalling, mediated by the elevated sFlt-1/PlGF ratio, had in turn an influence on LAT1 or NRF2. Indeed, *NFE2L2* and *SLC7A5* expression could be regulated just by modulating the sFlt-1/PlGF ratio (Fig. 4D). During PE-like conditions, i.e., Flt-1 OE and PlGF silencing, we saw a strong reduction of *NFE2L2* and *SLC7A5* levels and an increase in oxidative stress, i.e., a lowered GSH/GSSG ratio. However, when the opposite of a PE-phenotype by Flt-1 silencing and PlGF OE was simulated, *NFE2L2* and *SLC7A5* levels increased, and we were able to rescue the oxidative stress (Fig. 4D). Interestingly, *NFE2L2* was upregulated by both PlGF OE and silencing, while *SLC7A5* was increased by PlGF OE but not PlGF deficiency (Supplementary Fig. 13).

Finally, we wanted to demonstrate whether factors released by LAT1- and NRF2 deficient trophoblast cells can influence the viability of primary placental endothelial cells, i.e., PLECs. For this purpose, PLECs were treated with conditioned medium (CM) from LAT1- and NRF2-depleted HTR-8/SVneo cells, respectively. In comparison to controls, viability of PLECs decreased when treated with medium from LAT1- and NRF2 deficient cells; this in a similar manner (Fig. 4E). PLECs treated with CM extracts also showed decreased levels of *NFE2L2* and *SLC7A5* (Fig. 4F) and more oxidative stress (Fig. 4G). Comparable results in terms of lower viability and a reduced GSH/GSSG ratio were observed in PLECs treated with increasing (titrated) sFlt-1/PlGF ratios (Supplementary Fig. 14). We observed an upregulation of the sFlt-1/PlGF ratio in LAT1- and NRF2-depleted placental endothelial cells (PLECs) (Supplementary Fig. 15), similar as in HTR-8/SVneo cells (Fig. 3C).

Our data, showing that LAT1 and NRF2 regulate the sFlt-1/PlGF ratio, which in turn affects their expression, are summarised in our working model describing a new molecular mechanism involved in PE (Fig. 4H).

Discussion

We show here that LAT1 and NRF2 regulate one another to maintain cellular amino acid supply and redox status in balance. Even more relevant, this fundamental molecular mechanism is dysregulated in PE-derived placental cells.

Given that NRF2 regulates hundreds of genes[27] and some association studies suggest that LAT1 expression depends on NRF2[28,29], it is not surprising that LAT1 is among them. Nevertheless, LAT1 has not yet been confirmed as an NRF2 target gene. A very unexpected and counterintuitive finding was that LAT1 deficiency (which, as we show here, reduces amino acid uptake, leading to less GSH, and more oxidative stress in placental cells) led to downregulation of NRF2. Reduced uptake of methionine during LAT1 deficiency is of interest, because its demethylation into cysteine via the transsulfuration pathway has been identified as major contributor to GSH synthesis[18]. Cellular amino acid deficiency could activate ATF4 to restore amino acid levels[30]. Indeed, LAT1 deficient placental cells as well as placental cells that were starved for methionine upregulated ATF4 in a similar manner to PE-derived trophoblasts.

During PE, more sFlt-1 and less PlGF is produced, resulting in a higher sFlt-1/PlGF ratio[5]. Here we add a previously unknown function of ATF4, which is the promotion of *Flt1* expression. The incomplete mechanistic understanding of how ATF4 can simultaneously upregulate *Flt1* and downregulate *PGF* expression is a limitation of this study. ATF4 is known to transcriptionally inhibit some genes (e.g., PlGF[22]),

https://doi.org/10.1038/s41467-025-64160-0

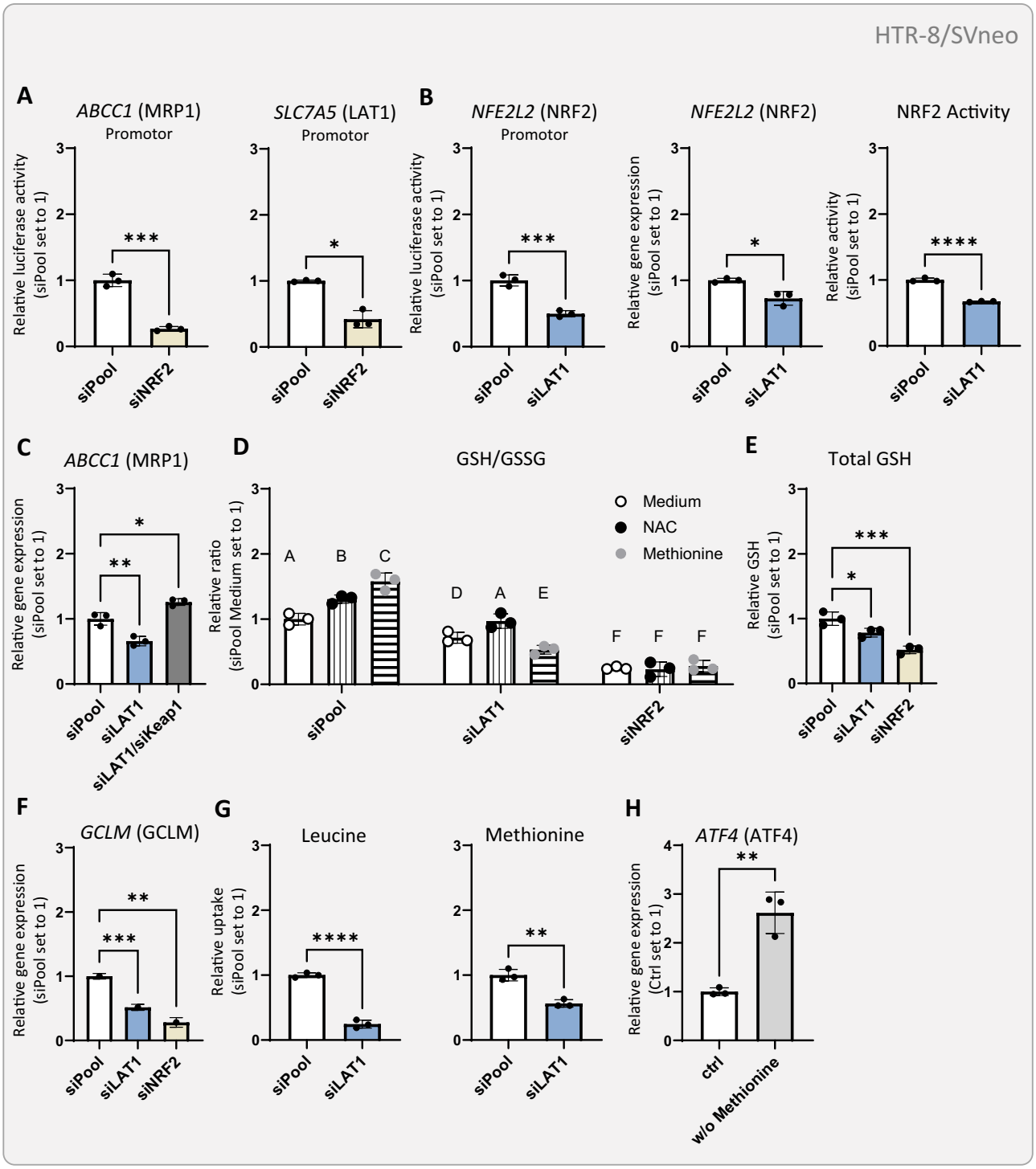

Fig. 2 | Mutual regulation of LAT1 and NRF2 affects oxidative stress and amino acid response of HTR-8/SVneo cells. A Promoter activity of *ABCC1* (MRP1) and *SLC7A5* (LAT1) after NRF2 depletion. **B** *NFE2L2* (NRF2) promoter activity and gene expression as well as nuclear NRF2 activity after LAT1 depletion. **C** *ABCC1* (MRP1) gene expression after LAT1, or concomitant LAT1 and Keap1 depletion. **D** GSH/GSSG ratio of cells treated with medium, medium + 90 mg/L methionine or +3 mM N-acetylcysteine (NAC) after siRNA-mediated silencing of *SLC7A5* (LAT1) and *NFE2L2* (NRF2). **E** Total cellular GSH in LAT1 and NRF2 deficient cells. **F** *GCLM* mRNA levels upon LAT1 and NRF2 depletion. **G** Relative leucine and methionine uptake in LAT1 and NRF2 deficient cells. **H** *ATF4* (ATF4) gene expression in cells cultured in control (ctrl) medium or methionine-free medium for 24 h. Data represent mean value ± SD. $N = 3$ (biological replicates). $^{*}P < 0.05$, $^{**}P < 0.01$, $^{***}P < 0.001$, $^{****}P < 0.0001$. Letters A–F denote homogeneous subgroups ($P < 0.05$) by post-hoc S-N-K test. Two-sided unpaired *t* test was used in (**A**, **B**, **G**, **H**). ANOVA followed by Dunnett´s multiple comparisons test was used in (**C**, **E**, **F**). ANOVA followed by S-N-K multiple comparisons test was used in (**D**).

while activating others[21]. This opposing regulation may involve distinct promoter elements, chromatin environments, or post-translational modifications of ATF4[21], which urges the need for further mechanistic studies.

Because ATF4 induction during LAT1 deficiency mediated an increased sFlt-1/PlGF ratio, we expected less free PlGF to trigger the phosphorylation and signalling of Flt-1. Accordingly, we found Akt, a Flt-1 downstream target[31], also reduced in LAT1 deficient cells.

https://doi.org/10.1038/s41467-025-64160-0

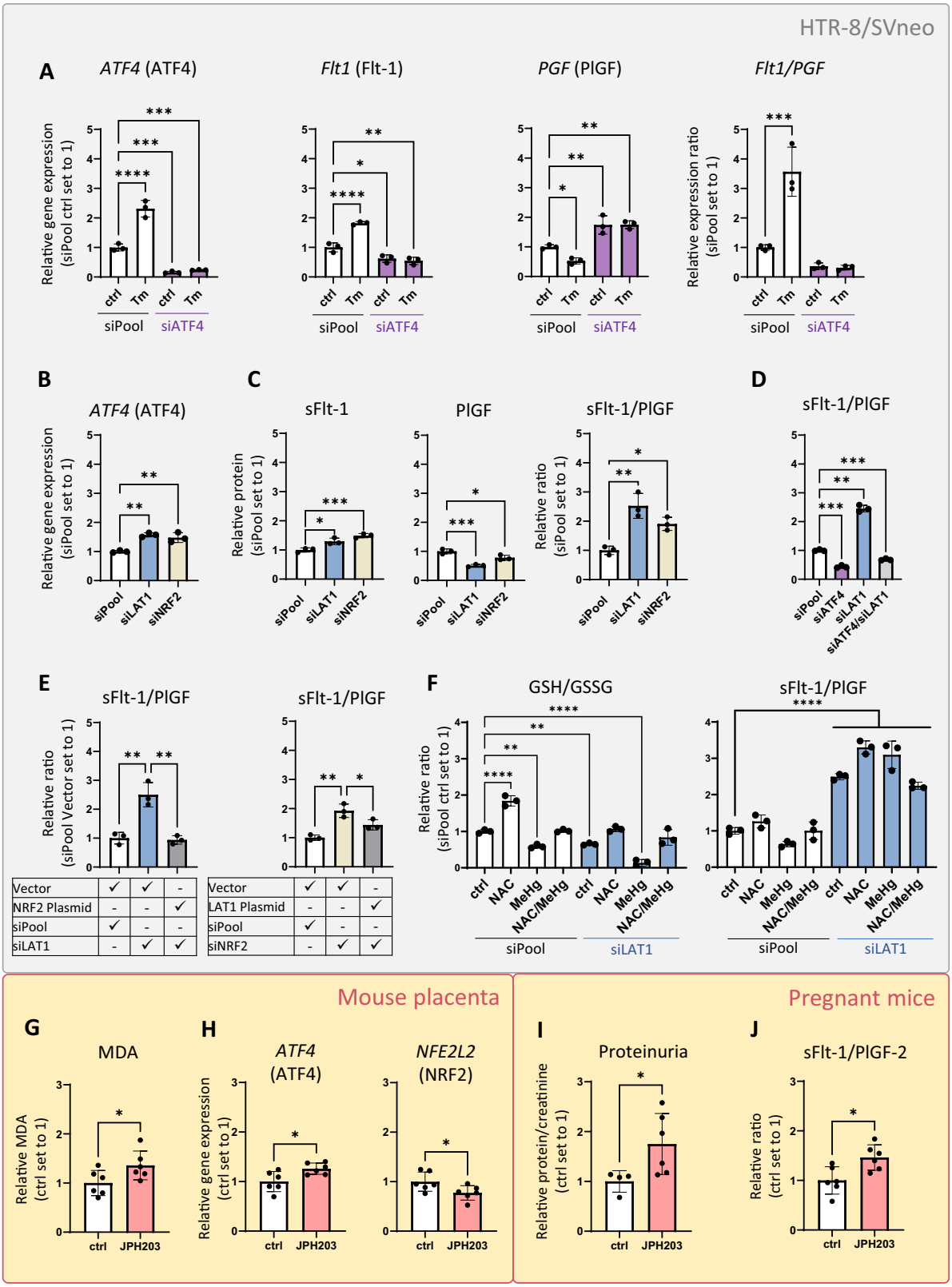

Phosphorylated Akt promotes NRF2 activation[32]. A decrease in NRF2 activity can be assumed to negatively affect its expression in a direct way (NRF2 promotes its own transcription[33]) and also an indirect manner (less LAT1 expression is followed by reduced NRF2 activation through Akt), ultimately explaining why we found NRF2 down-regulated after LAT1 silencing.

In addition to functional limitations, it is also conceivable that an underlying defect in LAT1 and/or NRF2 synthesis is involved in PE development. Several NRF2 gene sequence variants have been described to reduce NRF2 expression, increasing the risk for PE[34].

We here also show that during (MeHg-induced) oxidative stress PE-derived trophoblasts are significantly less able to upregulate LAT1

https://doi.org/10.1038/s41467-025-64160-0

Fig. 3 | Regulation of the sFlt-1/PlGF ratio during LAT1, and NRF2 deficiency. **A** Expression levels of *ATF4* (ATF4), *Flt1* (sFlt-1), and *PGF* (PlGF), as well as *Flt1/PGF* mRNA ratio in HTR-8/SVneo cells. Tm: Tunicamycin **B** ATF4 expression in LAT1- and NRF2 deficient cells. **C** Levels of sFlt-1 and PlGF in medium of LAT1 and NRF2 deficient cells, as well as the sFlt-1/PlGF ratio. **D** sFlt-1/PlGF ratio of cells deficient for ATF4, LAT1, or both proteins. **E** sFlt-1/PlGF ratio of cells deficient for LAT1 and NRF2 or overexpressing the proteins. **F** GSH/GSSG ratio and sFlt-1/PlGF ratio in LAT1 deficient cells treated with 0.9 μM methyl mercury (MeHg) and 3 mM N-acetylcysteine (NAC). **G** Malondialdehyde (MDA) levels in placentas obtained from control or JPH203 (LAT1 specific inhibitor) treated pregnant mice. **H** Gene expression levels of *ATF4* (ATF4) and *NFE2L2* (NRF2) in placentas obtained from control or JPH203- treated pregnant mice. **I** Proteinuria determined in urine of control or JPH203-treated mice that was collected immediately after sacrificing. **J** Ratio of sFlt-1/PlGF-2 in plasma of control or JPH203-treated mice (8- to 16-week-old naturally cycling females) that was collected immediately after sacrificing. Data represent mean value ± SD. **A**–**F**: $N = 3$ (biological replicates), **G**–**H** $N = 6$, **I** ctrl: $N = 4$; JPH203: $N = 6$, **J** $N = 6$; $^{*}P < 0.05$, $^{**}P < 0.01$, $^{***}P < 0.001$, $^{****}P < 0.0001$. ANOVA followed by Dunnett´s or Tukey´s multiple comparisons test was used in (**E**, **F**). Two-sided unpaired *t* test was used in (**G**–**J**).

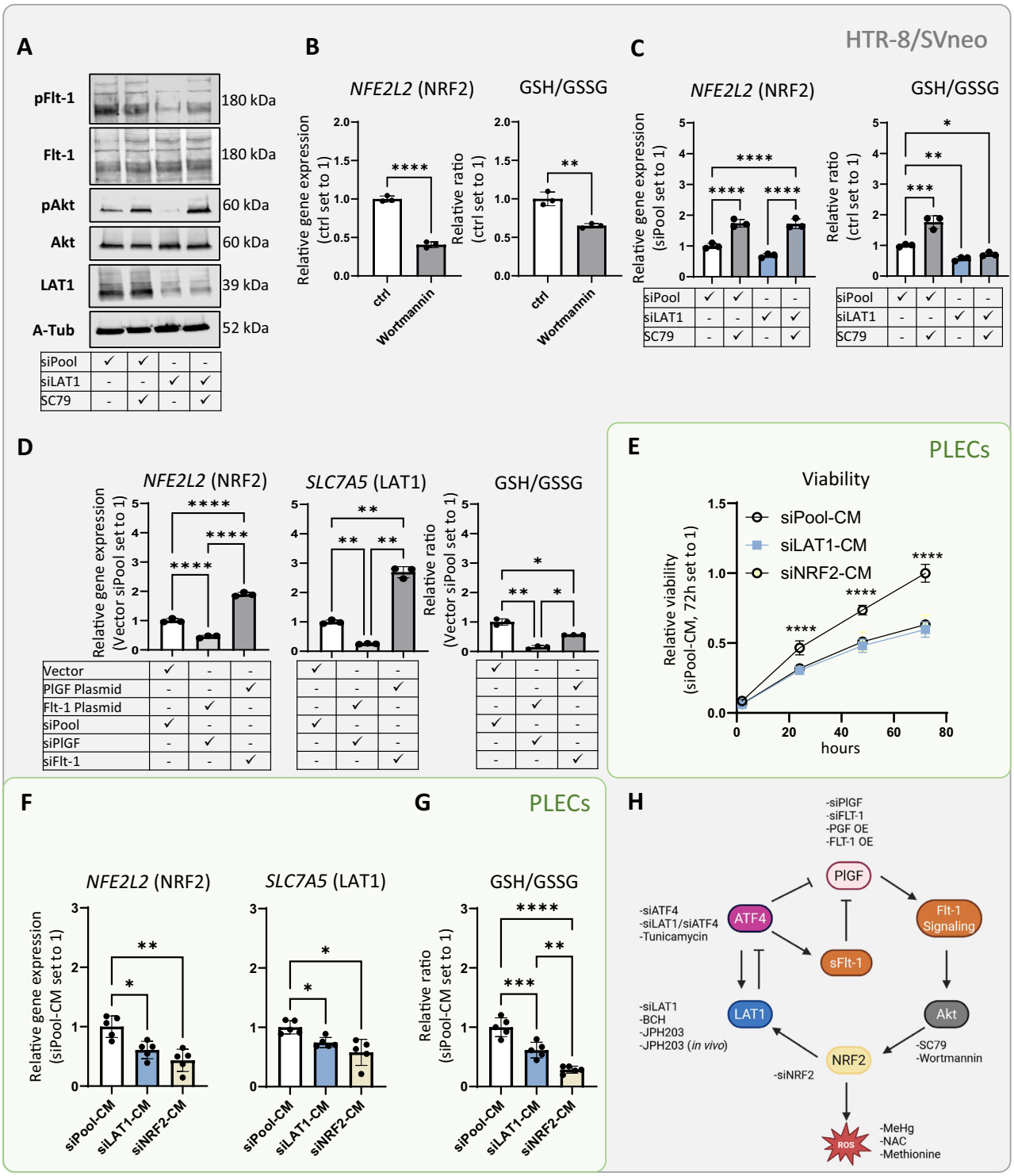

Fig. 4 | Flt-1 downstream signalling affects LAT1 and NRF2 signalling and cellular oxidative stress. A Immunoblots of phosphorylated and total Flt-1, phosphorylated and total Akt, LAT1, and alpha-tubulin (A-Tub) in control, LAT1 deficient and SC79 (Akt activator) treated cells. **B** *NFE2L2* (NRF2) mRNA levels and GSH/GSSG ratio in cells treated with Wortmannin **C** *NFE2L2* (NRF2) mRNA levels, and GSH/GSSG ratio in cells deficient of LAT1 or treated with SC79. **D** *NFE2L2* (NRF2) and *SLC7A5* (LAT1) mRNA levels, and GSH/GSSG ratio in cells overexpressing PlGF or Flt-1 that have been previously depleted of Flt-1 or PlGF, respectively. **E**–**G** Viability, *NFE2L2* (NRF2) and *SLC7A5* (LAT1) mRNA levels, and GSH/GSSG ratio of PLECs treated for 72 h with conditioned media (CM) from control (siPool), LAT1- and NRF2 deficient HTR-8/SVneo cells. **H** Proposed mechanism of the LAT1 and NRF2 interaction. LAT1 depletion causes amino acid deficiency and further activates ATF4. Activation of ATF4 upregulates Flt-1 (and also sFlt-1) and downregulates PlGF levels. This decreases Flt-1 signalling, causing less Akt-mediated NRF2 activation. Reduced NRF2 activity leads to lower levels of NRF2 itself, but also of its target genes including LAT1. This ultimately leads to more oxidative stress in the cell. The scheme describes the experimental steps underlying the working model, the circular nature of the mechanism, and that increased oxidative stress is a secondary effect of reduced NRF2 function and impaired amino acid uptake in PE placentas. In addition, as shown in Figs. 1I, 2, and Fig. 4A–D, LAT1 and NRF2 strongly correlate and interact regardless of whether PE is present or not. Created in BioRender. Gundacker, C. (2025) https://BioRender.com/boezau2 Data represent mean value ± SD. **A** The experiment was repeated at least three times with similar results. **B**–**D** $N = 3$ (biological replicates); **E**–**G** $N = 5$ (biological replicates). $^{*}P < 0.05$, $^{**}P < 0.01$, $^{***}P < 0.001$, $^{****}P < 0.0001$. Two-sided unpaired *t* test was used in (**B**). ANOVA followed by Dunnett´s or Tukey´s multiple comparisons test was used in (**C**–**G**).

and NRF2 gene expression in comparison to healthy hTCs. This is most likely a secondary effect due to reduced NRF2 function and supported by the fact that we were unable to induce the sFlt-1/PlGF ratio in HTR-8/SVneo cells by various oxidative stressors; only LAT1 or NRF2 deficiency could induce it. Our data strongly suggest that PE-associated oxidative stress, whose origin was unknown, is a secondary phenomenon caused by reduced NRF2 and LAT1 activity. However, because additional oxidative stress can put a great burden on a PE placenta, it is essential to avoid any oxidative stress-generating factors[35,36] during PE pregnancies.

Further studies on the effects of sFlt-1 and/or PlGF release from trophoblast cells on other placental cell types are needed to gain a better understanding of the long-term effects of PE on pregnant women and infants, who very often suffer from cardiovascular disease later in life. Conditioned medium from cultured placental villous explants, characterised by a higher sFlt-1/PlGF ratio, can induce endothelial dysfunction in HUVECs[37]. Here we show that induction of a higher sFlt-1/PlGF ratio by media extracts from LAT1- and NRF2 deficient trophoblast cells can directly reduce the viability of PLECs. Whether the susceptibility of endothelial cells to a higher sFlt-1/PlGF ratio is related to disturbances in angiogenic signalling, disturbances in the response to oxidative stress, or both, must be clarified in future research.

A better understanding of the molecular mechanisms behind PE could result in new treatments. In previous attempts to reduce the sFlt-1/PlGF ratio, the reduction of free sFlt-1[38] or the administration of additional PlGF[39] has been shown to ameliorate PE symptoms in mice. However, the protein ratio has to be tightly regulated, as excessive PlGF could also have adverse effects due to PlGF interference with other VEGF receptors such as VEGFR2[40].

PE is a multifactorial disease and cannot be attributed to a defect in a single protein. A circumstance that is clearly expressed in the mechanism proposed here. Accordingly, a defect in any step of the circular mechanism (e.g., due to maternal methionine deficiency, or impaired expression or function of one of the proteins involved) would ultimately lead to a PE-like phenotype.

Methods

Recruiting and sample collection

Pregnant women were recruited in the third trimester. Women aged 18–45 years who had given birth between gestational weeks 32 + 0 and 41 + 0 and provided written informed consent were included in the study. PE diagnosis was based on hypertension (systolic blood pressure ≥140 mmHg and/or diastolic blood pressure ≥90 mmHg), and/or proteinuria (proteinuria ≥300 mg/d or protein/creatinine quotient ≥30 mg/mmol) after the 20th week of pregnancy. Exclusion criteria were multiple pregnancy, maternal infections during pregnancy, pregestational hypertension, diabetes, thyroid dysfunction and substance abuse. Information on the study population are specified in Supplementary Tables 1 and 2. The study has been approved by the ethics committees (General Hospital Vienna vote no: EK 1035/2015; Clinics Lower Austria vote no: GS1-EK-4/305-2015).

Reagents

Detailed information on all reagents used during this study can be found in Supplementary Tables 3–9.

Animal studies

Wild-type C57BL/6J mice were purchased from Janvier Labs and housed at an animal facility of the Medical University of Vienna with constant temperature, air humidity and a 12-h light/12-h dark cycle. Regular chow diet and water have been provided ad libitum. The ethics of animal experimentation has been approved by the Ministry of Education, Science and Research (#2025-0.397.989) and conducted in strict accordance with FELASA guidelines. For timed-pregnancies, 8- to 16-week-old naturally cycling females were co-housed with wild-type males overnight. Successful mating was determined by the presence of a copulation plug the next morning and defined as gestational day 0.5 (GD0.5). For intravenous application, JPH203 dihydrochloride (GLPBio, dissolved in DMSO to a final concentration of 100 mg/ml) and vehicle control (DMSO) were diluted 1:5 in sterile PBS. Starting from GD14.5, pregnant females received daily intravenous treatments with JPH203 dihydrochloride (25 mg/kg body weight) or vehicle control for 3 consecutive days. Mice were sacrificed on GD17.5 and maternal blood, maternal urine, and placentas were collected for further analysis.

Placenta processing, mRNA isolation, cDNA synthesis, and quantitative PCR

Per human placenta, four tissue pieces (≤0.5 cm in any single dimension; according to Mayhew[41]) were submerged in 5–10 volumes of RNAlater® RNA Stabilization Solution (Life technologies) and stored at 4 °C for at least 24 h (or at −20 °C indefinitely). RNA extraction was performed using the PARIS procedure (Life technologies) according to the manufacturer's protocol. Two mouse placentas per litter were selected and homogenised and further processed as described above for human placentas.

Total RNA from cultured cells was isolated with TRI Reagent®(-Sigma) following manufacturer's instructions. About 1000 ng RNA from placental tissue or cells were reversely transcribed with Go-Script Reverse Transcription System Mix (Promega) using random hexamer primers. The cDNA was diluted 1:10, and 2 µL DNA were used in a 15 µL reaction to determine gene expression in an Applied Biosystems StepOnePlus™ Real-Time PCR System, according to the manufacturer's protocol.

Protein extraction and immunoblotting

Cells were lysed in Radio-Immunoprecipitation Assay lysis buffer (RIPA, Thermo Scientific) containing phosphatase and protease inhibitors. Supernatant containing soluble proteins were collected by

centrifugation at 15,000 × *g* for 15 min at 4 °C. Total protein concentration was determined by Bio-Rad Protein Assay and equal amounts of denatured samples were used for further analysis.

Proteins from placental tissue or cell pellets were resolved by SDS-PAGE and transferred to nitrocellulose membranes. Membranes were dried for 10 min at 37 °C and then blocked for 1 h in Odyssey Blocking Buffer (TBS) (LI-COR). Blots were incubated in primary antibody diluted in Odyssey Antibody Buffer (TBS) overnight at 4 °C. The following day, the blots were washed four times with TBS containing 0.1% Tween-20 (TBST) and incubated with the secondary fluorophore-conjugated antibody for 1 h at RT. The secondary antibody was detected with the Odyssey CLx imager (LI-COR) using Image Studio Lite 5.2 software. Equal loading of lysates was verified by detection of reference protein alpha-tubulin.

Isolation and cultivation of placental primary cells

hTCs were isolated from minced placental tissue with two cycles of trypsin (Gibco) and DNAse I (Sigma) digestion. Erythrocytes were removed with red blood cell lysis buffer (Roche) and the remaining cells were layered on top of a discontinuous 70-to-5% Percoll (GE Healthcare) density gradient. Cells banding between 1.048 and 1.062 g/ml were collected, washed, and resuspended in 1× Hanks balanced solution (ThermoFisher). Contaminating, human leukocyte antigen (HLA) class I-positive cells were removed using mouse-anti HLA class I antibody (Sigma) coupled to magnetic beads coated with goat anti-mouse immunoglobulin G (IgG) (Thermofisher). Cells were seeded at a density of 1×10^6 cells/ml in RPMI-1640 (10% fetal calf serum (FCS), 1% GlutaMax, 1% Penicillin/Streptomycin (Pen-Strep) (ThermoFisher), Keratinocyte Supplement Mix (ThermoFisher). hTCs were cultivated at 37 °C, 5% CO_2, and 95% humidity.

Arterial chorionic blood vessels at the apical surface of the chorionic plate were resected. Each vessel was washed with Hank's balanced salt solution (HBSS, Gibco) to remove residual blood. Vessels were perfused with prewarmed HBSS containing 0.1 U/ml collagenase, 0.8 U/ml dispase (Roche), and Pen-Strep (Gibco). PLECs suspension was centrifuged at 200 × *g* for 5 min, the pellet resuspended with EGM-MV medium (Promocell) and the cells seeded in flasks pre-coated with 1% gelatin (Sigma). PLECs were cultivated at 37 °C, 10% O_2, 5% CO_2, and 95% humidity.

Cultivation of HTR-8/SVneo cells

HTR-8/SVneo cells (ATCC, CRL-3271™, Lot# 64275781) were cultured in RPMI-1640 medium (Gibco), containing 5% fetal bovine serum (FBS; PanBiotech), 1% Glutamax (Gibco). Cells were grown at 37 °C, 5% CO_2, and 95% humidity and were routinely passaged with Accutase (Sigma) every 3-4 days at a ratio of 1:3 to 1:8.

The cell number was determined by CASY cell counter and analyzer (CASY® Model TTC 45/60/150, Innovatis Technologies Inc.). HTR-8/SVneo cells were periodically screened for the absence of mycoplasma (MycoAlert; Lonza). HTR-8/SVneo cell line identity and purity were verified by short tandem repeat (STR) profiling (ATCC).

Treatment of cells

Unless otherwise indicated, the standard dosages were 0.9 μM MeHg, 10 μM Menadione, 50 μM H_2O_2, and 100 μM buthionine sulfoximine (BSO). N-acetylcysteine (NAC) and methionine were applied at 3 mM and 90 mg/L, respectively. Furthermore, ATF4 activator (10 μg/L Tunicamycin), Akt activator (10 μM SC79) and Akt inhibitor (100 nM Wortmannin) were used.

Cell viability assay

Cell viability was measured in a 96-well multiplex format and determined by RealTime-Glo MT Cell Viability Assay (Promega) according to the manufacturer's protocol. In short, 1×10^3 cells/well were seeded and on the next day treated with MeHg and analysed at 2 h, 24 h, 48 h and 72 h post treatment. Assay performance, i.e., reduction of cell viability was controlled with 10 μM Ionomycin (Sigma).

siRNA mediated gene KD

HTR-8/SVneo cells, seeded in 6-well plates at a density of 1×10^5 cells/ml, were on the next day transiently transfected with nontargeting siRNA (siPool = controls) and target-specific siRNA using Lipofectamine RNAiMAX (ThermoFisher), as described previously[42]. A concentration of 50 nM siRNA was used in all experiments. Cells were cultured for 72 h before harvest.

Plasmid isolation and transfection

Plasmid was propagated in DH5α Chemically Competent E. coli cells (Origene) and isolated using the QIAGEN Plasmid Midi Kit according to the manufacturer's instructions. DNA concentration was determined using Nanodrop 1000. HTR-8/SVneo cells were seeded in 6-well plates at a density of 1×10^5 cells/ml. On the next day cells were transiently transfected with a control plasmid or target-specific plasmid using Turbofection 8.0 (Origene) in a ratio of 1 DNA: 3 Turbofectin 8.0. First, the plasmid DNA (2.5 μg/well) was pipetted into Opti-MEM (Thermofisher, 250 μl/well), mixed properly and then Turbofectin 8.0 (7.5 μl/well) was added and incubated at RT for 15 min. The transfection solution was then pipetted drop by drop into the well. The cells were incubated with the transfection mixture for 24 h, then the medium was changed, and the cells were incubated for further 24 h.

Reporter gene assay

HTR-8/SVneo were seeded in 96-well plates at a density of 1.5×10^4 cells/well. On the next day, cells were transiently transfected with luciferase reporter vectors of *NFE2L2* and *SLC7A5* using FugeneHD. For normalisation two reference genes (*ACTB, GAPDH*) were used. As negative control LightSwitch™ Random Promoter Control 2 was used. After 48 h of transfection, the plate was stored at −80 °C for 24 h. The next day the plate was thawed and the LightSwitch™ Luciferase Assay Kit was used to detect the reporter signal according to the manufacturer's protocol.

Amino acid uptake

HTR-8/SVneo cells (1×10^5 cells/ml) and hTCs (1×10^6 cells/ml) were cultured for 72 h, following incubation for 15 min in HBSS supplemented with either 0.38 mM leucine or 0.1 mM methionine (as found in the basal RPMI-1640 formulation). Each amino acid solution further contained radioactively labelled amino acids (1 μCi/mL L-[4,5-^{3} H(N)] Leucine (60 Ci/mmol, American Radiolabeled Chemicals, Inc.) or 1 μCi/mL L-[1-^{14} C] Methionine (55 mCi/mmol, American Radiolabeled Chemicals, Inc.)). For inhibitor experiments, cells were pretreated 24 h with 5 μM JPH203 (Selleckchem; according to ref. 43) or 1 mM BCH (R&D Systems; according to ref. 44). Comparability of treatment with JPH203 dihydrochloride or JPH203 was verified (Supplementary Fig. 16). 48 h after seeding, amino acid uptake was examined in the presence of the respective inhibitor. Afterwards, cells were washed three times with ice cold HBSS, followed by lysis in 250 μL 1 M NaOH (Merck) for 2 h at 37 °C. 200 μL cell lysate were added to 5 mL liquid scintillation fluid (Ultima Gold, Perkin Elmer) and radioactivity was determined by liquid scintillation counting (TRI-Carb 2800 TR, Perkin Elmer). Counts were normalised to protein content measured by Bradford reagent.

Mercury analysis

Samples and reference material were acid-digested with nitric acid (65%; suprapur) in a microwave oven (MARS6, CEM). Total mercury concentrations of cells were determined by CV-AFS (mercur plus, Analytik Jena). Quality assurance was achieved by measuring blank solutions (limit of detection was 0.4 μg/L) and reference material (Seronorm Trace Elements Human Whole Blood low level, Nycomed

LOT 1103129). The mean mercury level of three reference samples was 17.4 µg/L (recovery: 105 ± 4%). Mercury concentrations were normalised to cell number (HTR-8/SVneo) or protein content (hTCs).

Nucleus isolation and nuclear NRF2 activity assay

Nuclei were isolated with the Nuclear Extraction Kit (Abcam). In short, cells were detached using Accutase (Sigma), centrifuged at 350 × *g* for 5 min and the supernatant was discarded. Cell pellets were resuspended in 500 µl Pre-Extraction Buffer and incubated at 4 °C for 10 min. Cells were centrifuged at 12,000 × *g* for 1 min at 4 °C. Cytoplasmic fraction (supernatant) was pipetted into a reaction tube, and the nuclear pellet was stored at −80 °C for NRF2 activity assay.

Nuclear NRF2 activity was determined with NRF2 Transcription Factor Assay Kit (Abcam). In short, nuclear pellets were lysed in lysis buffer provided by the company. Concentration of nuclear protein was determined by Bio-Rad Protein Assay. 20 µg of nuclear extract/well was used to determine NRF2 activity in the nucleus. The assay was done according to the manufacturer's protocol.

Determination of the GSH/GSSG ratio

GSH/GSSG-Glo Assay (Promega), a luminescence-based system that quantifies total glutathione (GSH) and oxidised GSH (GSSG) in cultured cells, was used. Reduced GSH was calculated according to the manufacturer's protocol (total GSH − GSSG = reduced GSH). GSH levels were normalised to cell number.

ELISA

Human samples. sFlt-1 was quantified in cell culture supernatants in duplicates using Human VEGFR1/Flt-1 Quantikine ELISA Kit (R&D systems) according to the manufacturer's protocol. Cell culture supernatants were used undiluted to be within the detection range of the ELISA assay (0–2000 pg/ml). The concentrations of the reference material for Flt-1 (low: 220 ± 9.7 pg/ml; medium: 647 ± 21 pg/ml, high: 1430 ± 55 pg/ml) were well within the certified range (low: 140–249 pg/ml; medium: 417–751 pg/ml, high: 880–1519 pg/ml).

PlGF was quantified by Human PlGF Quantikine ELISA Kit according to the manufacturer's protocol. Cell culture supernatants were used undiluted within the detection range of the ELISA assay (0–1000 pg/ml). The concentrations of reference material for PlGF (low: 97 ± 12 pg/ml; medium: 300 ± 17 pg/ml, high: 567 ± 29 pg/ml) were well within the certified range (low: 64–132 pg/ml; medium: 189–331 pg/ml, high: 364–594 pg/ml).

Mouse samples. sFlt-1 was quantified using Mouse VEGFR1/Flt-1 ELISA Kit Quantikine (R&D systems) according to the manufacturer's protocol. Plasma was diluted 1:10 to be within the detection range of the ELISA assay (0–8000 pg/ml). The concentrations of the reference material for Flt-1 (972 ± 37 pg/ml) were well within the certified range 849–1414 pg/ml).

PlGF was quantified by Mouse PlGF-2 ELISA Kit Quantikine Kit according to the manufacturer's protocol. Plasma was diluted 1:2 to be within the detection range of the ELISA assay (0–1500 pg/ml). The concentrations of reference material for PlGF (145 ± 5 pg/ml) were well within the certified range (109–182 pg/ml).

MDA assay, mouse placenta

Lipid Peroxidation (MDA) assay (Sigma) was performed according to the manufacturer's protocol. One mouse placenta per litter was homogenised in the manufacturer's buffer and the results were normalised to placental weight. Here we used MDA as an oxidative stress marker, because the GSH/GSSG assay is not suitable for tissue.

Conditioned medium

24 h after KD, medium was replaced with fresh medium to remove free transfection aggregates. After further 48 h, conditioned medium from three six-well plates (three biological replicates) was concentrated with Amicon Ultro-15 (3 kDa) at 3500 × *g* for 60 min at 4 °C. Medium was pooled for treatment solutions and condensed to a tenth. PLECs at 50% density were treated for 72 h with MV medium supplemented with conditioned medium extract from LAT1 or NRF2 deficient HTR-8/SVneo cells. The experimental design is shown in Supplementary Fig. 17.

Proteinuria, mouse urine

Total protein was analysed by Nanodrop 1000 using the Protein 280 protocol. 2 µl urine were used undiluted to cover the detection range (0–100 mg/ml). Creatinine was determined using Creatinine Parameter Assay Kit (R and D Systems; KGE005). Samples were diluted 1:33 to cover the detection range (0–20 mg/dl). Proteinuria was determined by the ratio of total protein to creatinine in urine.

Statistics

GraphPad Prism 10, MS Excel and IBM SPSS 28 software were used in statistical analyses. The data represent mean values ± standard deviation (SD) from three or more independent experiments made in three technical replicates. Primary cells were isolated from at least five healthy and PE placentas, respectively. Two-group comparisons were done by two-sided unpaired *t*-test. One-way ANOVA and post-hoc analysis (Dunnett´s T3, Tukey´s or S-N-K) was used to compare multiple groups, and Spearman correlation analysis (R_s) was used for correlation analyses. The critical significance level was set at $\alpha = 0.05$, and *P* levels marked as $^{*}P < 0.05$, $^{**}P < 0.01$, $^{***}P < 0.001$, $^{****}P < 0.0001$. The representatively selected immunoblots originate from independently repeated experiments. The statistical analyses of individual experiments are available in the source data.

Reporting summary

Further information on research design is available in the Nature Portfolio Reporting Summary linked to this article.

Data availability

Data generated in the study are provided in the Supplementary Information and Source Data files. Source data are provided with this paper.

References

1. Burton, G. J., Redman, C. W., Roberts, J. M. & Moffett, A. Pre-eclampsia: pathophysiology and clinical implications. *BMJ* **366**, l2381 (2019).
2. Huppertz, B. Biology of preeclampsia: Combined actions of angiogenic factors, their receptors and placental proteins. *Biochim. Biophys. Acta Mol. Basis Dis.* **1866**, 165349 (2020).
3. Kweider, N. et al. A possible protective role of Nrf2 in preeclampsia. *Ann. Anat.* **196**, 268–277 (2014).
4. Dimitriadis, E. et al. Pre-eclampsia. *Nat. Rev. Dis. Prim.* **9**, 8 (2023).
5. Zeisler, H. et al. Predictive value of the sFlt-1:PlGF ratio in women with suspected preeclampsia. *N. Engl. J. Med.* **374**, 13–22 (2016).
6. Chau, K., Hennessy, A. & Makris, A. Placental growth factor and pre-eclampsia. *J. Hum. Hypertens.* **31**, 782–786 (2017).
7. Maynard, S. E. et al. Excess placental soluble fms-like tyrosine kinase 1 (sFlt1) may contribute to endothelial dysfunction, hypertension, and proteinuria in preeclampsia. *J. Clin. Invest.* **111**, 649–658 (2003).
8. Huang, Z., Huang, S., Song, T., Yin, Y. & Tan, C. Placental angiogenesis in mammals: a review of the regulatory effects of signaling pathways and functional nutrients. *Adv. Nutr.* **12**, 2415–2434 (2021).
9. Pollheimer, J., Vondra, S., Baltayeva, J., Beristain, A. G. & Knofler, M. Regulation of placental extravillous trophoblasts by the maternal uterine environment. *Front. Immunol.* **9**, 2597 (2018).

10. Aouache, R., Biquard, L., Vaiman, D. & Miralles, F. Oxidative stress in preeclampsia and placental diseases. *Int. J. Mol. Sci.* **19**, https://doi.org/10.3390/ijms19051496 (2018).
11. Dinkova-Kostova, A. T., Hakomaki, H. & Levonen, A. L. Electrophilic metabolites targeting the KEAP1/NRF2 partnership. *Curr. Opin. Chem. Biol.* **78**, 102425 (2024).
12. Panieri, E., Telkoparan-Akillilar, P., Suzen, S. & Saso, L. The NRF2/KEAP1 axis in the regulation of tumor metabolism: mechanisms and therapeutic perspectives. *Biomolecules* **10**, https://doi.org/10.3390/biom10050791 (2020).
13. Dickinson, D. A. & Forman, H. J. Glutathione in defense and signaling: lessons from a small thiol. *Ann. N. Y. Acad. Sci.* **973**, 488–504 (2002).
14. Lennicke, C. & Cocheme, H. M. Redox metabolism: ROS as specific molecular regulators of cell signaling and function. *Mol. Cell* **81**, 3691–3707 (2021).
15. Tantengco, O. A. G. et al. The role of nuclear factor erythroid 2-related factor 2 (NRF2) in normal and pathological pregnancy: a systematic review. *Am. J. Reprod. Immunol.* **86**, e13496 (2021).
16. Forman, H. J., Zhang, H. & Rinna, A. Glutathione: overview of its protective roles, measurement, and biosynthesis. *Mol. Aspects Med.* **30**, 1–12 (2009).
17. Straka, E. et al. Mercury toxicokinetics of the healthy human term placenta involve amino acid transporters and ABC transporters. *Toxicology* **340**, 34–42 (2016).
18. McBean, G. J. The transsulfuration pathway: a source of cysteine for glutathione in astrocytes. *Amino Acids* **42**, 199–205 (2012).
19. Ouyang, Y., Wu, Q., Li, J., Sun, S. & Sun, S. S-adenosylmethionine: a metabolite critical to the regulation of autophagy. *Cell Prolif.* **53**, e12891 (2020).
20. Rasmussen, B. B. & Adams, C. M. ATF4 is a fundamental regulator of nutrient sensing and protein turnover. *J. Nutr.* **150**, 979–980 (2020).
21. Neill, G. & Masson, G. R. A stay of execution: ATF4 regulation and potential outcomes for the integrated stress response. *Front. Mol. Neurosci.* **16**, 1112253 (2023).
22. Mizuuchi, M. et al. Placental endoplasmic reticulum stress negatively regulates transcription of placental growth factor via ATF4 and ATF6beta: implications for the pathophysiology of human pregnancy complications. *J. Pathol.* **238**, 550–561 (2016).
23. Graham, C. H. et al. Establishment and characterization of first trimester human trophoblast cells with Supplementary lifespan. *Exp. Cell Res.* **206**, 204–211 (1993).
24. Simmons-Willis, T. A., Koh, A. S., Clarkson, T. W. & Ballatori, N. Transport of a neurotoxicant by molecular mimicry: the methylmercury-L-cysteine complex is a substrate for human L-type large neutral amino acid transporter (LAT) 1 and LAT2. *Biochem. J.* **367**, 239–246 (2002).
25. Hoffmeyer, R. E. et al. Molecular mimicry in mercury toxicology. *Chem. Res. Toxicol.* **19**, 753–759 (2006).
26. Granitzer, S. et al. Amino acid transporter LAT1 (SLC7A5) mediates mehg-induced oxidative stress defense in the human placental cell line HTR-8/SVneo. *Int. J. Mol. Sci.* **22**, https://doi.org/10.3390/ijms22041707 (2021).
27. Song, M. Y., Lee, D. Y., Chun, K. S. & Kim, E. H. The role of NRF2/KEAP1 signaling pathway in cancer metabolism. *Int. J. Mol. Sci.* **22**, https://doi.org/10.3390/ijms22094376 (2021).
28. Valdovinos-Flores, C. et al. Systemic L-buthionine -S-R-sulfoximine treatment increases plasma NGF and upregulates L-cys/L-cys2 transporter and gamma-glutamylcysteine ligase mRNAs through the NGF/TrkA/Akt/Nrf2 pathway in the striatum. *Front. Cell Neurosci.* **13**, 325 (2019).
29. Purbey, P. K. et al. Defined sensing mechanisms and signaling pathways contribute to the global inflammatory gene expression output elicited by ionizing radiation. *Immunity* **47**, 421–434 e423 (2017).
30. Kilberg, M. S., Shan, J. & Su, N. ATF4-dependent transcription mediates signaling of amino acid limitation. *Trends Endocrinol. Metab.* **20**, 436–443 (2009).
31. Wang, F. et al. RACK1 regulates VEGF/Flt1-mediated cell migration via activation of a PI3K/Akt pathway. *J. Biol. Chem.* **286**, 9097–9106 (2011).
32. Zou, W. et al. PI3K/Akt pathway mediates Nrf2/ARE activation in human L02 hepatocytes exposed to low-concentration HBCDs. *Environ. Sci. Technol.* **47**, 12434–12440 (2013).
33. Bryan, H. K., Olayanju, A., Goldring, C. E. & Park, B. K. The Nrf2 cell defence pathway: Keap1-dependent and -independent mechanisms of regulation. *Biochem. Pharm.* **85**, 705–717 (2013).
34. Khadir, F., Rahimi, Z., Ghanbarpour, A. & Vaisi-Raygani, A. Nrf2 rs6721961 and oxidative stress in preeclampsia: association with the risk of preeclampsia and early-onset preeclampsia. *Int. J. Mol. Cell Med.* **11**, 127–136 (2022).
35. Li, B., Qiao, C., Jin, X. & Chan, H. M. Characterizing the low-dose effects of methylmercury on the early stages of embryo development using cultured human embryonic stem cells. *Environ. Health Perspect.* **129**, 77007 (2021).
36. Widhalm, R. et al. Perfluorodecanoic acid (PFDA) increases oxidative stress through inhibition of mitochondrial beta-oxidation. *Environ. Pollut.* **367**, 125595 (2025).
37. O'Brien, M., Baczyk, D. & Kingdom, J. C. Endothelial dysfunction in severe preeclampsia is mediated by soluble factors, rather than extracellular vesicles. *Sci. Rep.* **7**, 5887 (2017).
38. Bergmann, A. et al. Reduction of circulating soluble Flt-1 alleviates preeclampsia-like symptoms in a mouse model. *J. Cell Mol. Med.* **14**, 1857–1867 (2010).
39. Spradley, F. T. et al. Placental growth factor administration abolishes placental ischemia-induced hypertension. *Hypertension* **67**, 740–747 (2016).
40. Caporale, A. et al. Short PlGF-derived peptides bind VEGFR-1 and VEGFR-2 in vitro and on the surface of endothelial cells. *J. Pept. Sci.* **25**, e3146 (2019).
41. Mayhew, T. M. Taking tissue samples from the placenta: an illustration of principles and strategies. *Placenta* **29**, 1–14 (2008).
42. Rosner, M. et al. Efficient siRNA-mediated prolonged gene silencing in human amniotic fluid stem cells. *Nat. Protoc.* **5**, 1081–1095 (2010).
43. Enomoto, K. et al. A novel therapeutic approach for anaplastic thyroid cancer through inhibition of LAT1. *Sci. Rep.* **9**, 14616 (2019).
44. Kim, C. S. et al. BCH, an inhibitor of system L amino acid transporters, induces apoptosis in cancer cells. *Biol. Pharm. Bull.* **31**, 1096–1100 (2008).

Acknowledgements

We wish to thank the study participants, Florian Frommlet (Center for Medical Data Science, Medical University of Vienna) for statistical advice, and the medical staff for organisational support. Graphics were created with BioRender.com. This study was supported by GFF (Gesellschaft für Forschungsförderung Niederösterreich m.b.H.) under Project No. LS15-014; (C.G., H.S.).

Author contributions

S.G., R.W., C.G., M.H., M.R. conceptualized and designed experiments. S.G., R.W., L.M., P.E., M.F. performed experiments. S.G., R.W., C.G., M.H., M.R., I.E. interpreted data. H.S., H.Z., P.F., E.G. coordinated the clinical part of the study. S.G., R.W., C.G. wrote the manuscript. M.H., C.G., H.S., T.W., G.S., H.Z., G.D., M.K., L.S. supplied resource and funding.

Competing interests

The authors declare no competing interests.

Additional information

Supplementary information The online version contains supplementary material available at https://doi.org/10.1038/s41467-025-64160-0.

Correspondence and requests for materials should be addressed to Claudia Gundacker.

Peer review information *Nature Communications* thanks the anonymous reviewers for their contribution to the peer review of this work. A peer review file is available.